Front. Phys., 2011, 6(1): 96–99
DOI 10.1007/s11467-010-0154-z

RESEARCH ARTICLE

First-principle investigation of the electronic and magnetic properties of $PbMn(SO_4)_2$

Fang WU (吴芳)[1,†], **Er-jun KAN** (阚二军)[2], **Zhen-yu LI** (李震宇)[3]

[1] *School of Science, Nanjing Forestry University, Nanjing 210037, China*

[2] *Department of Applied Physics, Nanjing University of Science and Technology, Nanjing 210094, China*

[3] *Hefei National Laboratory for Physical Sciences at the Microscale, University of Science and Technology of China, Hefei 230026, China*

E-mail: [†] *fangwu@mail.ustc.edu.cn*

Received September 21, 2010; accepted October 20, 2010

The magnetic properties of oxide $PbMn(SO_4)_2$ consisted of MnO_6 octahedra which connected with each other through SO_4 tetrahedra, are well studied in experiments. In this paper, we explored its interesting electronic and magnetic properties with first-principle calculations. Our results show that all Mn ions have high spin states, namely, $S = 5/2$, and the magnetic couplings between NN and NNN are antiferromagnetic, which agree well with the experimental results. Besides, the surprising results of spin exchange interactions between the NN and NNN are excellently explained with extended Hückel tight-binding calculations.

Keywords first-principle calculations, magnetic properties, spin exchange

PACS numbers 71.15.Mb, 71.20.Be, 75.47.Lx

1 Introduction

The crystal structure of the magnetic oxide $PbMn(SO_4)_2$ was first studied by West *et al.* [1]. As illustrated in the Fig. 1, the distorted octahedra MnO_6 are connected with each other through the SO_4 tetrahedra. The chain formed by the Mn^{2+} ions along a direction alternate with the chain of the Pb^{2+} ions along b direction. Besides the crystal structure, West *et al.* also reported the magnetic properties of $PbMn(SO_4)_2$ by using the powder x-ray and neutron diffraction [1]. According to their investigation, $PbMn(SO_4)_2$ undergoes antiferromagnetic (AFM) three-dimensional (3D) order below ~ 5.5 K (i.e., $T_N \approx 5.5$ K). The Curie–Weiss temperature θ of $PbMn(SO_4)_2$, reported to be -10.7 K, shows that dominant AFM interactions exist. Since T_N is considerably smaller than $|\theta|$(i.e., $|\theta|/T_N \approx 2$), substantial geometric spin frustration [2, 3] should be present in $PbMn(SO_4)_2$.

After checking the atomic environment, we found that each Mn^{2+} ion has four nearest neighbors (NN) Mn^{2+} ions, and they are connected by the double Mn–O–S–O–Mn path ways. On the other hand, each Mn^{2+} ion is also surrounded by four next nearest neighbors (NNN) Mn^{2+} ions and connected by a single Mn–O–S–O–Mn path way. However, the nature and strength of the spin exchange interactions between the NN and NNN of Mn^{2+} ions have not been determined so far. To our knowledge, the strengths of J_1, J_2 between the NN and NNN are the super-super exchange (SSE) interactions and proportional to Curie–Weiss temperature θ. The relationship

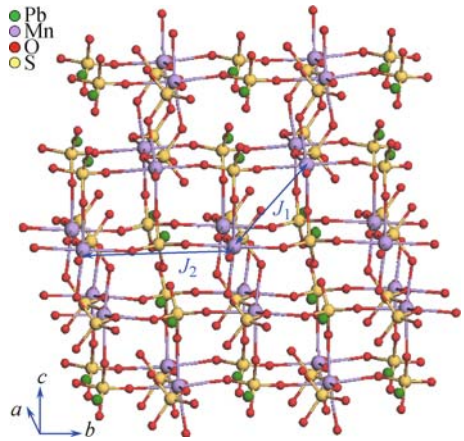

Fig. 1 Structural features of $PbMn(SO_4)_2$: MnO_6 octahedra connected with each through SO_4 tetrahedra. Mn^{2+} and Pb^{2+} ions form chains along the a direction and the chains are alternative along the b direction. The green, pink, red and yellow circles represent the Pb, Mn, O and S atoms, respectively. J_1 and J_2 are two spin exchanges.

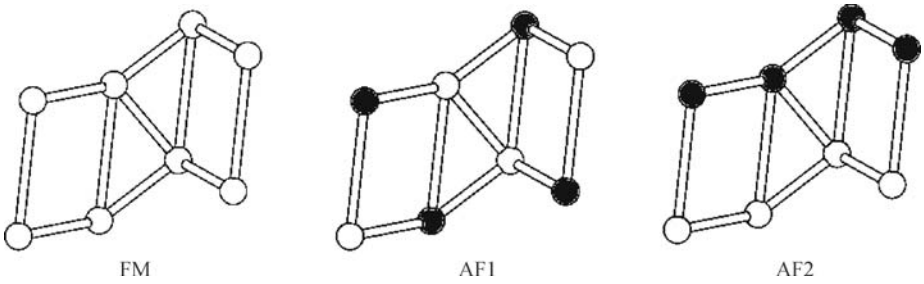

Fig. 2 Three ordered spin states of $PbMn(SO_4)_2$ employed to extract the spin exchanges J_1–J_2 by mapping analysis based on density functional calculations, where the unshaded and shaded circles represent the Mn^{2+} ions with up-spin and down-spin, respectively.

between the Curie–Weiss temperature θ and the spin exchanges can be described as: $\theta = \frac{S(S+1)}{3k_B}\sum_i z_i J_i$ [4], where the summation runs over all nearest neighbors of a given spin site, z_i is the number of nearest neighbors connected by the spin exchange parameter J_i, and S is the spin quantum number of each spin site (i.e., $S = 5/2$ in the present case). In terms of the experimental Curie–Weiss temperature θ (−10.7 K), we can predict that the strength of SSE J_1 and J_2 should be very weak, and the stronger one should be AFM.

In order to investigate the novel properties of $PbMn(SO_4)_2$, we theoretically study the electronic and magnetic properties of $PbMn(SO_4)_2$ for the first time through electronic calculations and evaluating the spin exchange interactions by employing the mapping analysis based on density functional electronic structure calculations [5–12]. To extract the values of J_1, J_2 on the basis of density functional calculations, three ordered spin states of $PbMn(SO_4)_2$ are adopted, as depicted in Fig. 2.

2 Computational method

Our spin-polarized density functional calculations employed the projector augmented wave method implemented in Vienna *ab initio* simulation package [13–15] with the generalized gradient approximation (GGA) [16] for the exchange-correlation functional, the plane-wave cutoff energy of 400 eV, a set of $5 \times 2 \times 2$ points [17], and the threshold 10^{-5}eV for energy convergence. In general, the electron correlation associated with 3d states is not well described by density functional calculations, and this deficiency is commonly corrected by using the GGA plus on-site repulsion U (GGA+U) method. Considering the electron correlation of Mn 3d, we carried out GGA+U calculations with $U = 3.0$ eV [18, 19].

3 Results and discussion

Figure 3 shows plots of the total density of states (DOS) and the projected DOS (PDOS) for the Mn 3d states, obtained from GGA+U (U = 3.0 eV) calculations for the ferromagnetic (FM) state of $PbMn(SO_4)_2$. As we can see, the band gap is predicted to be about 2.5 eV by the GGA+U calculations. All up-spin Mn 3d states are occupied and are separated with a band gap from the all down-spin states lying above. This is consistent with the finding that $PbMn(SO_4)_2$ consists of high-spin Mn^{2+} (d^5) ions and is a magnetic insulator.

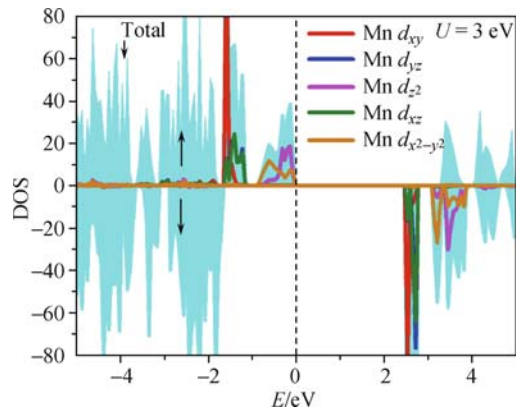

Fig. 3 Plots of the total DOS and the PDOS for the Mn 3d states obtained for the FM state of $PbMn(SO_4)_2$ from the GGA + U calculations with $U = 3.0$ eV on Mn.

For the magnetic properties of $PbMn(SO_4)_2$, the accurate spin exchange parameters are needed. To determine the values of J_1, J_2, we express the energies of the three ordered spin states in terms of the spin Hamiltonian,

$$\hat{H} = -\sum_{i<j} J_{ij}\hat{S}_i \cdot \hat{S}_j \quad (1)$$

in which J_{ij} (= J_1, J_2) is the exchange parameter for the interaction between the spin sites i and j, while $\hat{S}_i$ and $\hat{S}_j$ are the spin angular momentum operators at the spin sites i and j, respectively. By applying the energy expressions obtained for spin dimers with N unpaired spins per spin site (in the present case, $N = 5$ [20, 21]), the total spin exchange energies (per formula unit) of the three ordered spin states are written as:

$$E_{FM} = (-2J_1 - 2J_2)\frac{N^2}{4} \quad (2)$$

$$E_{AF1} = (+J_1)\frac{N^2}{4} \quad (3)$$

$$E_{\mathrm{AF2}} = (-J_2)\frac{N^2}{4} \quad (4)$$

The relative energies of the three ordered spin states of $PbMn(SO_4)_2$ (Fig. 2), obtained from our GGA+U (with $U = 3.0$ eV), are summarized Table 1. Therefore, the values of J_1–J_2 listed in Table 2 are determined by equating the relative energies of the three ordered spin states obtained from GGA+U calculations to the corresponding relative energies obtained from the total spin exchange energies.

Table 1 Relative energies (in meV) of the three ordered spin states obtained from GGA+U ($U = 3.0$ eV) calculation.

E_{FM}	E_{AF1}	E_{AF2}
0	−3.96	−3.56

Table 2 Spin exchange parameters J_1–J_2 (in K) obtained from GGA+U calculation.

J_1(k)	J_2(k)
−0.36	−3.13

From the spin exchange values of Table 2, the following are observed: (i) As we expect in the introduction, the spin interactions J_1, J_2 between the Mn^{2+} ions are very weak because of the low Neél temperature. (ii) In the GGA+U calculations, both of J_1 and J_2 spin interactions are AFM exchanges, and the stronger one is J_2. As we know, antiferromagnetic exchanges are inversely proportional to the electronic correction U value, which means larger U will reduce the spin interactions. But the general picture that J_2 is stronger than J_1 will not be changed by the U value. In our studies, we have adopted U value as 3 eV, which is reasonable for 3d transition metal atoms, and the results agree well with the observed experimental data. Thus, our results should be reliable. (iii) In the GGA+U calculations, the AFM exchanges J_1, J_2, J_1 triangles lead to spin frustration.

It is well known that the local octahedral distortions have important consequences on the nature and strength of the spin exchanges. Therefore, we present geometrical parameters associated with the spin exchange paths J_1–J_2 in Table 3. As we can see, the <M–O–O and <O–O–M angles of the SSE paths J_1 and J_2 are greater than 90. Therefore, the magnetic orbitals of Mn ions can overlap with each other, resulting in the AFM coupling [22]. Both of SSE J_1 and J_2 are involving Mn–O···O–Mn paths in $PbMn(SO_4)_2$, and J_1 has a shorter Mn–Mn distance than J_2 (4.943 Å vs. 6.733 Å). Nevertheless, the strength of an SSE interaction M–O···O–M, where M is a magnetic transition-metal ion, is essentially determined by the overlapping between the O orbtials. In general, the O orbital overlapping depends on the O···O contact distance and is expected to become strong when the O···O contact distance is short. Table 3 indicates that J_2 has a slightly shorter O···O contact distance than does the J_1 (2.377 Å vs. 2.435 Å or 2.407 Å). It is not surprising that the strength of J_2 is larger than J_1, but unbelievable that J_2 is more than eight times of J_1.

Table 3 Geometrical parameters associated with the spin exchange paths J_1–J_2. The lengths are in Å, and the angles in degrees.

	Mn···Mn	Mn–O···O–Mn	<Mn–O···O, <O···O–Mn
J_1	4.943	2.161, 2.435, 2.194	117.52, 114.84
		2.234, 2.417, 2.161	
J_2	6.733	2.194, 2.377, 2.234	161.55, 171.31

To get more clear pictures about the magnetic coupling, we use the extended Hückel tight-binding calculations to analyze the calculated spin exchange parameters. In this part, we will explain why the super-superexchange (SSE) J_2 is much stronger than J_1. To explain this apparently surprising result, we determine the magnetic orbitals of the $Mn_2O_{16}S_2$ and $Mn_2O_{14}S$ involving the J_1 and J_2 SSE paths by extended Hückel tight-binding calcaulations. As presented in Fig. 4, magnetic orbitals of Mn_2O_{12} are composed of the anti-bonding Mn 3d and O 2p orbtials. The overlapping of O 2p orbitals involving the spin exchange path J_1 is almost zero because the O 2p orbitals are perpendicular to each other, while the overlapping of O 2p orbitals becomes much stronger because of the parallel O 2p orbitals involving the spin exchange path J_2. Generally speaking, AFM spin exchange J depends on the overlap of magnetic orbitals, and J_{AF} becomes negligible if the overlap integral

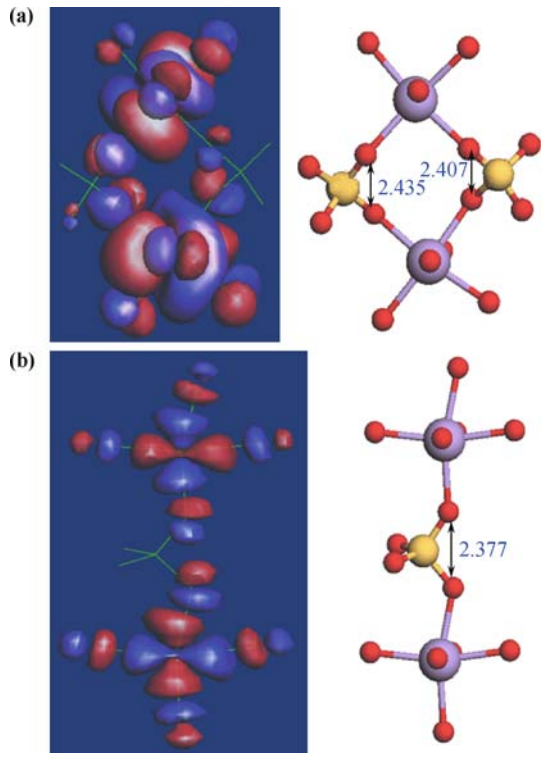

Fig. 4 Shapes of the magnetic orbitals of the Mn_2O_{12} obtained from extended Hückel tight-binding calculations. **(a)** Arrangement of two Mn_2O_{12} octahedra in the spin exchange J_1; **(b)** Arrangement of two Mn_2O_{12} octahedra in the spin exchange J_2.

between the magnetic orbitals is small. Therefore, the spin exchange J_2 is strongly AFM because of the large overlapping, other than the geometrical distance.

4 Conclusion

We have performed comprehensive first-principle calculations to investigate the electronic and magnetic properties of $PbMn(SO_4)_2$. Our results show that all Mn ions have high spin states, namely, $S = 5/2$. The magnetic properties are studied based on the spin exchanges J_1–J_2 of $PbMn(SO_4)_2$ extracted from first-principle calculations. Both J_1 and J_2 are AFM, and J_2 is much stronger than J_1, and J_1, J_2, J_1 triangles lead to spin frustration which is consistent with the experiment result. Besides, the intrinsic mechanic leading to the stronger J_2 is well explored with extended Hückel tight-binding calcaulations.

Acknowledgements The work at Nanjing Forestry University was supported by the Science Funding for High-qualified Talents of the University (Grant No. 163070047). The work at University of Science and Technology of China (USTC) was supported by the USTC-HP HPC project, and the SCCAS and Shanghai Supercomputer Center.

References

1. D. V. West, I. D. Posen, Q. Huang, H. Zandbergen, T. Mcqueen, and R. Cave, J. Solid State Chem., 2009, 182: 2461
2. J. E. Greedan, J. Mater. Chem., 2001, 11: 37
3. D. Dai and M.-H. Whangbo, J. Chem. Phys., 2004, 121: 672
4. J. S. Smart, Effective Field Theory of Magnetism, Philadelphia: Saunders, 1966
5. M.-H. Whangbo, H. Koo, and D. Dai, J. Solid State Chem., 2003, 176: 417
6. M.-H. Whangbo, D. Dai, and H. Koo, Solid State Sci., 2005, 7: 827
7. H. Koo, M.-H. Whangbo, P. VerNooy, C. Torardi, and W. Marshall, Inorg. Chem., 2002, 41: 4664
8. H. Koo and M.-H. Whangbo, Inorg. Chem., 2008, 47: 128
9. H. Koo and M.-H. Whangbo, Inorg. Chem., 2008, 47: 4779
10. J. Kang, C. Lee, R. Kremer, and M.-H. Whangbo, J. Phys.: Condens. Matter, 2009, 21: 392201
11. F. Wu, E. Kan, and M.-H. Whangbo, Inorg. Chem., 2010, 49: 3025
12. F. Wu, E. Kan, and M.-H. Whangbo, Inorg. Chem., 2010, 49: 7545
13. G. Kresse and J. Hafner, Phys. Rev. B, 1993, 62: 558
14. G. Kresse and J. Furthmüller, Comput. Mater. Sci., 1996, 6: 15
15. G. Kresse and J. Furthmüller, Phys. Rev. B, 1996, 54: 11169
16. J. P. Perdew, S. Burke, and M. Ernzerhof, Phys. Rev. Lett., 1996, 77: 3865
17. S. L. Dudarev, G. A. Botton, S. Savrasov, C. Humphreys, and A. Sutton, Phys. Rev. B, 1998, 57 : 1505
18. E. Kan, L. F. Yuan, and J. L. Yang, J. Appl. Phys., 2007, 102: 033915
19. S. Ji, E. Kan, M.-H. Whangbo, J.-H. Kim, Y. Qiu, M. Matsuda, H. Yoshida, Z. Hiroi, M. A. Green, T. Ziman, and S.-H. Lee, Phys. Rev. B, 2010, 81: 094421
20. D. Dai and M. -H. Whangbo, J. Chem. Phys., 2001, 114: 2887
21. D. Dai and M. -H. Whangbo, J. Chem. Phys., 2003, 118: 29
22. J. B. Goodenough, Magnetism and the Chemical Bond, New York: Wiley Interscience, 1963